Available online at www.sciencedirect.com
ScienceDirect
Journal of Photochemistry and Photobiology A: Chemistry 192 (2007) 130–141
Journal of Photochemistry and Photobiology A:Chemistry
www.elsevier.com/locate/jphotochem

Photochromism of 1,2-*bis*(2-methyl-5-phenylthien-3-yl) perfluorocyclopentene in liposomes

Yili Bai, Kristen M. Louis, R. Scott Murphy *

Department of Chemistry and Biochemistry, University of Regina, 3737 Wascana Parkway, Regina, SK S4S 0A2, Canada

Received 18 September 2006; received in revised form 23 March 2007; accepted 16 May 2007
Available online 18 May 2007

Abstract

A photochromic dithienylethene, 1,2-*bis*(2-methyl-5-phenylthien-3-yl)perfluorocyclopentene (**1**), was synthesized and incorporated into the lipid bilayer of liposomes as a strategy for demonstrating the potential for complete photocontrol over the permeability of a lipid membrane. Absorption spectroscopy and differential scanning calorimetry (DSC) were used to characterize the photochromism and inclusion of **1** in dipalmitoylphosphatidylcholine (DPPC) large unilamellar liposomes (LUVs), respectively. Absorption studies confirm that the photoisomerization of **1** in DPPC LUVs is completely reversible, although hindered due to the more restrictive and rigid environment posed by the lipid bilayer. DSC studies strongly suggest that **1** is partially buried in the hydrocarbon core of the bilayer, interacting primarily with the C2–C8 methylene region of the acyl chains of DPPC. Photoinduced changes in the membrane permeability of DPPC LUVs were assessed by monitoring changes in the fluorescence of an encapsulated fluorophore, 8-hydroxypyrene-1,3,6-trisulfonic acid (HPTS), upon photocycling **1** between the two photoisomers using ultraviolet and visible light. The fluorescence studies show that release of encapsulated HPTS is not observed following the irradiations. Thus, the photoisomerization of **1** does not lead to a large disruption in the local lipid order within the bilayer.

Keywords: Dithienylethene; Liposome; Photochromism; Photoisomerization; Quantum efficiency

1. Introduction

The design of drug delivery systems with controls (e.g. dosage, targeting) is an ambitious goal for many pharmaceutical and academic research laboratories. The formulation of new and more efficient ways to administer therapeutics to specific areas of the body is in constant development. Liposomes, or lipid vesicles, are spherical self-enclosed structures composed of biodegradable, nontoxic phospholipids. These supramolecular assemblies have been recognized for their potential utility as drug delivery vehicles since the 1970s [1]. However, only recent developments in this field have finally produced liposomal products that are either in advanced clinical trials, or have been approved for clinical use [1–3]. In spite of this, their delivery strategies with respect to controlling the amount of encapsulated drug that is released over a specific time interval (i.e. dosage) remains extremely limited and passive. As a result, slow release kinetics can significantly reduce the efficacy of the drug delivery methodology.

An active triggering mechanism such as the use of light as a stimulus to induce changes in the permeability of a lipid membrane (i.e. permeable versus nonpermeable) is a dynamic area of research [4]. Phototriggering can significantly enhance control over release kinetics from liposomes with high spatial and temporal resolution through the use of modern laser systems coupled to optical fibers so that *in vivo* excitation is not limited to surface tissues. Thus, far, much of the focus has been on the study of irreversible phototriggers such as photopolymerization [5,6] which are unable to regulate dosage. Reversible photocontrols based on the isomerization of photochromic azobenzene [7,8], spiropyran [9–11], and spirooxazine [12] derivatives have been studied in lipid membranes. However, a disadvantage with many azobenzene systems is the overlapping absorption of isomers in the ultraviolet (UV) region, which hinders selective excitation especially in systems containing multiple chromophores. Although this drawback is less problematic for the spiropyran and spirooxazine systems, thermal reversibility and low fatigue resistance limits the application of these photochromic

* Corresponding author. Tel.: +1 306 585 4247; fax: +1 306 337 2409.
E-mail address: scott.murphy@uregina.ca (R. Scott Murphy).

1010-6030/$ – see front matter © 2007 Elsevier B.V. All rights reserved.
doi:10.1016/j.jphotochem.2007.05.016

systems in drug delivery. To achieve complete photocontrol over the release of encapsulated compounds from liposomes, these limitations will have to be addressed. A thermally irreversible system will allow for improved photoregulation of the delivered dosage. As a first step towards this goal the photochromic dithienylethene, 1,2-*bis*(2-methyl-5-phenylthien-3-yl)perfluorocyclopentene (**1**), has been chosen. In addition to the thermal irreversibility and high fatigue resistance of **1**, the absorption spectra for the open- (**1o**) and closed-ring (**1c**) isomers are well separated (Chart 1). This family of photochromic compounds is well known for their optoelectronic properties [13–15] and has been studied in various matrices [16–18], but they have never been characterized in liposomes.

We have synthesized and incorporated **1** into the lipid bilayer of a liposome as a strategy for demonstrating the potential for complete photocontrol over the permeability of a lipid membrane. Before employing synthetically more challenging dithienylethene derivatives with complementary lipid-like structures that will potentially cause a greater disruption to the lipid bilayer, it is important to establish that **1** is included in the lipid bilayer, determine its relative location within the membrane, and show that its photochromism is conserved. In this study, we have characterized the inclusion and photoisomerization of **1** in liposomes. In addition, we have evaluated the effect of the photoisomerization of **1** on membrane permeability and show that release of encapsulated compounds is not observed following UV and visible irradiations. This supports our hypothesis that the photoisomerization of **1** does not lead to a large disruption in the local lipid order within the bilayer. To conclude, the prospect of using more complementary dithienylethene derivatives to photoregulate the permeability of a lipid membrane in liposomes is discussed.

2. Experimental

2.1. Synthesis

2.1.1. Instrumentation

^{1}H NMR spectra were obtained at 200 MHz on a Bruker AC200 QNP spectrometer (Milton, ON, Canada). Mass spectra were recorded on a Finnigan Mat Incos 50 quadrupole mass spectrometer (Waltham, MA, USA) interfaced via a heated transfer line/capillary to a Hewlett-Packard 5890 gas chromatograph (Palo Alto, CA, USA). The gas chromatograph was configured with a splitless injection port and a DB-5MS fused-silica capillary column coated with a 0.25 μm film of stationary phase (15 m, 0.25 mm i.d.). The mass spectrometer was operated in the electron impact ionization mode with an electron energy of 70 eV. The ion source temperature was maintained at 180 °C for all analyses, and the capillary interface transfer line was held at 250 °C. All analyses were performed using a full scan mode resulting from 2 μL injections.

2.1.2. Materials

All reactants (>99%, Aldrich, Oakville, ON, Canada), deuterated solvents (99.9 atom %D, Aldrich), tetrakis(triphenyl -phosphine)palladium(0) ([$Pd^0(PPh_3)_4$]) (>99.9%, Strem Chemicals, Newburyport, MA, USA), and octafluorocyclopentene (>99%, SynQuest Laboratories, Alachua, FL, USA) were used as received. Diethyl ether and tetrahydrofuran were distilled prior to use. Preparative thin-layer chromatography (TLC) was carried out on aluminum-backed ALUGRAM SIL G/UV254 plates (Rose Scientific, Edmonton, AB, Canada) and visualized by a 6 W UVAC-18 dual wave (365/254 nm) UV handheld lamp from UltraLum (Claremont, CA, USA). Flash column chromatography was performed on silica gel (200–400 mesh, 60 Å, Aldrich).

2.1.3. Synthetic methods

*2.1.3.1. 3,5-Dibromo-2-methylthiophene (**3**).* The bromination of 2-methylthiophene (**2**) was adapted from known procedures [13,16,19] as shown (Scheme 1). To an ice cooled solution of **2** (8.53 g, 87 mmol) in acetic acid (35 mL, 142 mmol), a solution of bromine (10 mL, 195 mmol) in acetic acid (150 mL, 610 mmol) was added dropwise over a period of 45 min. The reaction mixture was stirred for a further 16 h at room temperature, and then poured into water (100 mL). It should be noted that initial attempts following literature procedures resulted in reaction mixtures that quickly turned dark brown and eventually to a black thick oil. We believe this polymerized product was due to the high concentration of bromine suggested from earlier reports. We modified these procedures by reducing the reported bromine concentration by two-fold. The brown oil was separated and the water phase was extracted with ether. The combined organic phases were washed with 0.1 M sodium bicarbonate solution and dried over calcium chloride. Upon reduced pressure distillation (bp 98.5 °C, 10 mmHg) [19], **3** was obtained in a 70% yield (15.12 g). ^{1}H NMR ($CDCl_3$, δ): 6.8 (s, 1H, ArH), 2.3 (s, 3H, CH_3).

*2.1.3.2. 3-Bromo-2-methyl-5-thiopheneboronic acid (**4**).* Lithiation and subsequent electrophilic substitution of **3** was adapted from known procedures [13,16,19]. To a stirred mixture of **3** (7.22 g, 28 mmol) in anhydrous diethyl ether (200 mL)

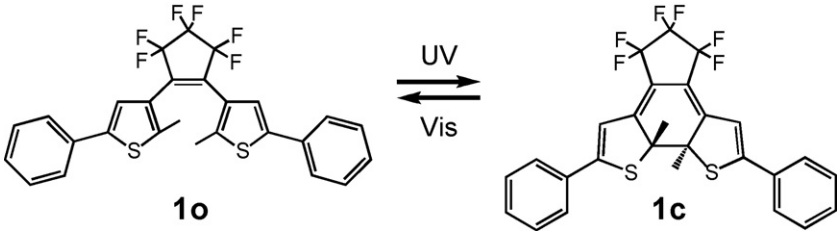

Chart 1.

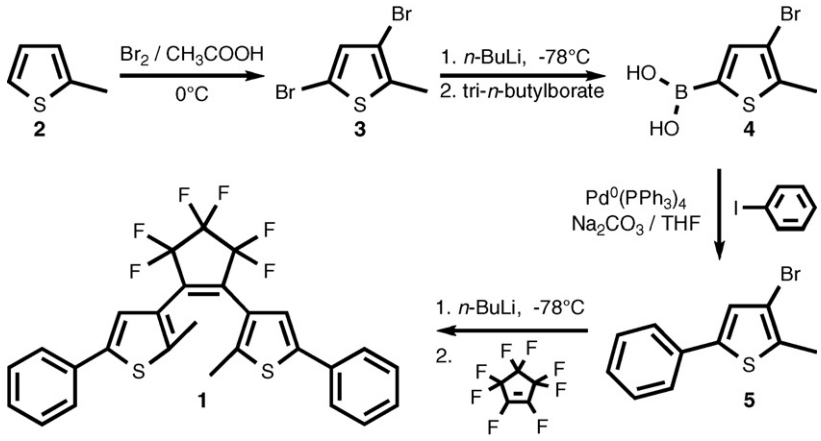

Scheme 1.

cooled in a dry ice–acetone bath (−78 °C), *n*-butyllithium (12 mL, 30 mmol, 2.5 M in hexane) was added under a nitrogen atmosphere. After 30 min, tri-*n*-butyl borate (11 mL, 42 mmol) was added. The reaction was stirred at −78 °C for 4 h and then allowed to warm to room temperature. After 15 h, the reaction mixture was quenched with diluted hydrochloric acid (100 mL, 1.2 M) and the organic phase was extracted with sodium hydroxide (4 × 28 mL, 1.0 M). The combined aqueous phases were filtered to remove traces of solid, and then acidified to pH 1 at 0 °C with concentrated hydrochloric acid. The resulting precipitate was filtered, washed with diluted hydrochloric acid (10 mM), and dried under vacuum. Compound **4** was obtained in a 40% yield (2.40 g) as a white powder. ^{1}H NMR (DMSO-d_6, δ): 2.4 (s, 3H, CH_3), 7.48 (s, 1H, ArH), 8.33 (s, 2H, OH).

*2.1.3.3. 3-Bromo-2-methyl-5-phenylthiophene (**5**).* The palladium-catalyzed Suzuki coupling of **4** and iodobenzene was adapted from known procedures [13,16,19,20]. In a glove bag, a mixture of **4** (1.33 g, 6.0 mmol) with iodobenzene (1.22 g, 6.0 mmol) was added to mixture of [$Pd^0(PPh_3)_4$] (0.21 g, 0.18 mmol) and sodium bicarbonate solution (5 mL, 0.30 M) in anhydrous tetrahydrofuran (45 mL). The reaction mixture was stirred at 70 °C for 6 h under a nitrogen atmosphere. The crude product was purified by column chromatography (hexanes). Compound **5** was obtained in a 50% yield (1.14 g) as a white powder. ^{1}H NMR ($CDCl_3$, δ): 2.41 (s, 3H, CH_3), 7.10 (s, 1H, ArH), 7.33–7.51 (m, 5H, ArH).

*2.1.3.4. 1,2-bis(2-Methyl-5-phenylthien-3-yl)perfluorocyclopentene (**1**).* The coupling of **5** to perfluorocyclopentene was adapted from known procedures [13,16,19]. To a stirred solution of **5** (1.01 g, 4 mmol) in 15 mL anhydrous tetrahydrofuran, *n*-butyllithium (1.7 mL, 4 mmol, 2.5 M in hexane,) was added dropwise in a dry ice–acetone bath (−78 °C) under a nitrogen atmosphere. Stirring was continued for 20 min and then perfluorocyclopentene (0.42 g, 2 mmol) was slowly added. The reaction mixture was stirred for another 3 h and then quenched by the addition of methanol. The product was extracted with ether, and the organic layer was washed with both 1 M hydrochloric acid and water. The organic layer was dried over magnesium sulfate, filtered, and solvent was removed under reduced pressure. The crude product was purified by column chromatography (1:3 toluene:hexanes) and recrystallized from hexane three times. Compound **1o** was obtained in a 23% yield (0.23 g) as a colorless powder. ^{1}H NMR ($CDCl_3$, δ): **1o**: 1.97 (s, 6H, CH_3), 7.28 (s, 2H, ArH), 7.2–7.6 (m, 10H, ArH); **1c**: 2.18 (s, 6H, CH_3), 6.68 (s, 2H, ArH), 7.3–7.7 (m, 10H, ArH). GC–MS *m/z* (% relative intensity, ion): 520 (100, M^+), 521 (31.1, M+1), 522 (13.4, M+2), 523 (3, M+3), 524 (0.5, M+4). UV ($CHCl_3$) λ_{max} (nm): **1o**: 280; **1c**: 310, 380, 580.

2.2. Liposome studies

2.2.1. General

A SB20 pH meter with a saturated calomel electrode from VWR (Edmonton, AB, Canada) was used to measure the pH of buffer stock solutions at constant temperature (20.0 ± 0.5 °C). The Mini-Extruder, 1 mL gas-tight syringes, 0.4, 0.2, and 0.1 μm polycarbonate membrane filters, and filter supports used for liposome extrusion were purchased from Avanti Polar Lipids (Alabaster, AL, USA). PD-10 desalting columns containing Sephadex G-25 M medium, purchased from Amersham Biosciences (Baie d'Urfe, QC, Canada), were used to remove unencapsulated and unincorporated compounds. A Rayonet RPR-100 photochemical reactor (Southern New England Ultraviolet Company, Branford, CT, USA) equipped with eight 8 W UVA lamps from Luzchem (Ottawa, ON, Canada) was used as the UV irradiation source. These broadband lamps have an emission maximum at 350 nm with a FWHM of ca. 30 nm. The visible (vis) irradiation source was a 100 W incandescent bulb. Infrared radiation was filtered with a Pyrex beaker containing cool water. All samples were irradiated in Pyrex test tubes from Fisher Scientific (Ottawa, ON, Canada) and measured in 10 mm × 10 mm quartz SUPRASIL absorbance or fluorescence cells from Hellma (Concord, ON, Canada).

2.2.2. Instrumentation

The phase transition temperatures of the liposomes were measured using a differential scanning calorimeter (DSC) Q-

10 from TA Instruments (New Castle, DE, USA). The radii of the liposomes were measured using a DAWN EOS multi-angle laser light scattering instrument from Wyatt Technology Corporation (Santa Barbara, CA, USA). Steady-state absorption spectra were obtained at constant temperature (20.0 ± 0.2 °C) on a Cary 100 Bio UV–vis spectrophotometer (Mississauga, Ont., Canada) equipped with a dual cell Peltier circulator accessory. The absorption spectra were corrected for the baseline spectrum of HEPES buffer and recorded at a scan rate and step size of 300 nm/min and 0.5 nm, respectively. Steady-state fluorescence spectra were obtained at constant temperature (20.0 ± 0.2 °C) using a PTI QM-2 spectrofluorimeter (London, ON, Canada). The excitation and emission slits were set to optimize the emission intensity, typically with a bandpass of 2 nm, and the excitation wavelength and integration time were set to 413 nm and 0.25 s, respectively.

2.2.3. Materials

1,2-Dipalmitoyl-*sn*-glycero-3-phosphocholine (DPPC) (> 99%, Avanti Polar Lipids), melittin (95%, Aldrich), *p*-xylene-*bis*-pyridinium dibromide (DPX) (>99%, Invitrogen, Burlington, Ont., Canada), 4-(2-hydroxyethyl)piperazine-1-ethanesulfonic acid (HEPES) (>99.5%, Aldrich), ethylenediaminetetraacetic acid, disodium salt (EDTA) (>99%, Aldrich), phenanthroline (>99%, Aldrich), sodium chloride (NaCl) (99%, EMD Chemicals, Gibbstown, NJ, USA), and Triton X-100 (scintillation grade, Eastman Kodak Company, Rochester, NY, USA) were used as received. 8-Hydroxypyrene-1,3,6-trisulfonic acid trisodium salt (HPTS) (dye content ≈ 75%, Aldrich) was recrystallized from ethanol three times. All aqueous solutions were prepared in pH 7.25 HEPES buffer (10 mM HEPES, 145 mM NaCl, 0.1 mM EDTA, $NaHCO_3$), and deoxygenated with argon (UHP grade, Praxair, Mississauga, Ont., Canada) for at least 15 min. Potassium ferrioxalate was synthesized following known procedures [21], and was recrystallized from water three times prior to use. Deionized water was obtained from a D8991 NANOpure Infinity water system from Barnstead (Dubuque, IA, USA). All organic solvents were of the highest available commercial grade.

2.2.4. Preparation of large unilamellar vesicles (LUVs)

The preparation of LUVs for membrane permeability studies was adapted from known procedures [1,22]. Four separate stock solutions of DPPC and **1** in chloroform (1.36 mM and 1.92 mM, respectively) and HPTS and DPX in HEPES buffer (10 mM and 100 mM, respectively) were prepared. The HPTS–DPX (10 mL) stock solution to be encapsulated in LUVs was prepared by combining HPTS (3.0 mL) DPX (1.8 mL), and HEPES buffer (5.2 mL) to give a HPTS:DPX mole ratio of 1:6. The preparation of DPPC LUVs (sample A) and those containing **1** (sample B), HPTS–DPX (sample C), or both (sample D) followed similar procedures varying only in the addition of these compounds in the appropriate amounts. To prepare sample A (ca. 3 mL, ca. 0.4 mM), DPPC stock solution (1.10 mL) was added to a 10 mL round bottom flask and then the chloroform was evaporated under reduced pressure to deposit a dry lipid film. The sample was dried under vacuum overnight and then hydrated with HEPES buffer (0.60 mL). Both buffer and the flask containing the dry lipid film were preheated at 50 °C. The sample was allowed to hydrate for at least 3 h at 50 °C and then overnight at 3 °C. The hydrated lipid suspension underwent 3–5 freeze and thaw cycles by placing the sample in a dry ice–acetone bath followed by a warm water bath. Extrusion was preformed at constant temperature (50.0 ± 0.5 °C) using 0.4 μm membrane filters. The gas-tight syringes were prewetted with buffer solution and the sample was extruded 10 times to give ca. 0.5 mL of sample. The preparation of sample B differs from sample A only in the addition of **1** (0.23 mL) to DPPC (1.10 mL) prior to deposition of the lipid film to give a **1**:DPPC mole ratio of 1:3. Similarly, sample C differs only in the addition of HPTS–DPX (0.60 mL) instead of HEPES buffer during hydration. Sample D includes both of these changes. Following extrusion, all samples (2.5 mL, 0.5 mM) were diluted with buffer loaded onto buffered desalting columns, and eluted with 3.5 mL of buffer to remove unencapsulated HPTS–DPX. The first 10 drops of eluent were discarded to give a purified LUV sample (ca. 3 mL, ca. 0.4 mM).

2.2.5. Preparation of multilamellar vesicles (MLVs)

The preparation of MLVs for DSC studies was adapted from known procedures [1,22]. DPPC MLVs and those containing **1** at mole ratios of 1:4, 1:3 and 1:2 (**1**:DPPC) followed similar procedures varying only in the addition of **1** in the appropriate amounts. To prepare pure DPPC MLVs (0.20 mL, 27 mM), DPPC stock solution (4.0 mL) was added to a 10 mL round bottom flask and then the chloroform was evaporated under reduced pressure to deposit a dry lipid film. The sample was dried under vacuum overnight and then hydrated with HEPES buffer (0.20 mL). Both buffer and the flask containing the dry lipid film were preheated to 50 °C. The sample was allowed to hydrate for at least 2 h at 50 °C and occasionally vortexed. The preparation of DPPC MLVs containing **1** differs only in the addition of **1** (0.7, 1.0 and 1.3 mL) with DPPC (4.0 mL) prior to deposition of the lipid film to give a **1**:DPPC mole ratio of 1:4, 1:3 and 1:2, respectively.

2.2.6. Lamellarity studies

A melittin stock solution (100 μM) was prepared by dissolving melittin (0.07 mg) in methanol (250 μL). Following LUV preparation protocols, a DPPC LUV sample encapsulated with HPTS–DPX was prepared (ca. 3 mL, ca. 0.7 mM). Two aliquots (0.75 mL, samples A and B) of this sample were transferred into two identical fluorescence cells. Aliquots of the melittin stock solution (10 μL) were transferred to sample A and fluorescence spectra were recorded before and after each addition. This was repeated until the fluorescence intensity at 510 nm (I_{Total}) reached a plateau. Then the total volume of melittin required to reach this plateau was added to sample B in one aliquot, the fluorescence spectrum was recorded, and the emission intensity (I_{LUV}) was obtained. The ratio of LUVs to the total liposome mixture was calculated as I_{LUV}/I_{Total}.

2.2.7. Multi-angle light scattering (MALS) studies

Following LUV preparation protocols, two DPPC LUV samples were prepared (12 and 15 ppm). The 12 and 15 ppm samples

were extruded through 0.2 and 0.4 μm membrane filters, respectively. Serial dilution of these samples with HEPES buffer was performed to give two sets of six samples (4.0 mL each) with a range of DPPC concentrations (0.2 μm = 2, 4, 6, 8, 10, and 12 ppm; 0.4 μm = 2.5, 5, 7.5, 10, 12.5, and 15 ppm). Each sample within one set was individually analyzed starting with the lowest concentration of DPPC. The samples were loaded into the flow cell of the MALS instrument using a syringe pump set at 20 mL/h and measured at constant temperature (25.0 ± 0.1 °C).

2.2.8. Quantum efficiency studies

The relative quantum efficiency for the ring-closing reaction of **1** in DPPC LUVs was determined by comparing its quantum efficiency to **1** in hexane. The quantum efficiency of a reaction is defined as the ratio of the number of molecules of product formed to the total number of photons absorbed, in the spectral region used, during the reaction period [23]. To determine the photon rate for our experimental setup that includes a polychromatic UV source (Rayonet RPR-100 photochemical reactor containing eight 8 W UVA lamps with an emission maximum at 350 nm with a FWHM of ca. 30 nm) a chemical actinometer, potassium ferrioxalate, was employed. The preparation of solutions and procedures for determining the photon rate have been well described [24]. Briefly, a 3 mL aliquot of a 0.012 M solution of ferrioxalate (6 g of potassium ferrioxalate in 1 L of 0.05 M sulfuric acid) was transferred to a 10 mm × 10 mm quartz cell and irradiated for 30 s, whereas an identical sample was placed in the dark. Following the irradiation, 0.05 mL of a buffered phenanthroline solution (0.1%: 225 g sodium acetate, 1 g of phenanthroline in 1 L of 0.5 M sulfuric acid) was added to both cells and the absorbance of the tris–phenanthroline complex at 510 nm was measured immediately. The moles of ferrous ions formed during the irradiation interval was determined using Eq. (1),

$$\text{moles Fe}^{2+} = \frac{V_1 \times V_3 \times \Delta A\,(510\,\text{nm})}{V_2 \times l \times \varepsilon\,(510\,\text{nm})} \quad (1)$$

where V_1 is the irradiated volume, V_2 the aliquot of the irradiated solution taken for the determination of the ferrous ions, V_3 the final volume after complexation with phenanthroline, l the optical pathlength of the quartz cell, ΔA (510 nm) the difference in absorbance between the irradiated and dark samples, and ε (510 nm) is the molar absorptivity of the $Fe(phen)_3^{2+}$ complex ($\varepsilon = 11100\,M^{-1}\,cm^{-1}$). Further, the photon rate or moles of photons absorbed by the irradiated solution per unit time ($Nh\nu/t$) was determined using Eq. (2),

$$\frac{Nh\nu}{t} = \frac{\text{moles Fe}^{2+}}{\phi \times t} \quad (2)$$

where ϕ is the quantum yield of ferrous ion production for the irradiation wavelengths used ($\phi = 1.21$), and t is the irradiation time (30 s). For our experimental setup, a photon rate of $(2.096 \pm 0.056) \times 10^{-8}$ mol/s was obtained from six independent experiments. To determine the moles of **1** that were converted to the ring-closed form upon irradiation with UV light, samples of **1** in hexane and 100 nm DPPC LUVs of equivalent concentration were prepared and irradiated with UV light. In addition, a ferrioxalate sample was always irradiated under identical experimental conditions. The quantum efficiency (η) of **1** in hexane and DPPC LUVs was determined using Eq. (3),

$$\eta = \frac{\Delta A\,(575\,\text{nm}) \times V}{(Nh\nu/t) \times \varepsilon\,(575\,\text{nm}) \times t} \quad (3)$$

where ΔA (575 nm) is the difference in absorbance between the irradiated and dark samples, V the irradiated volume, $Nh\nu/t$ the photon rate ($(2.096 \pm 0.056) \times 10^{-8}$ mol/s), ε (575 nm) the molar absorptivity of the ring-closed form of **1** in hexane ($\varepsilon = 15600\,M^{-1}\,cm^{-1}$ [16]), and t is the irradiation time (30 s). The quantum efficiency of **1** in DPPC LUVs was then compared with that obtained for **1** in hexane to determine the relative quantum efficiency for the ring-closing reaction of **1** in DPPC LUVs. Note that this ratio represents a lower limit for the relative quantum efficiency because a proportion of the total number of photons incident on the quartz cell are scattered by the LUVs. To obtain an upper limit for the relative quantum efficiency the proportion of incident light scattered by LUVs was determined. A 10 mm × 5 mm quartz cell containing a sample of LUVs was positioned between the UV light source and a 10 mm × 10 mm quartz cell containing ferrioxalate solution, whereas an identical ferrioxalate sample was placed in the dark. In this way, the 5 mm cell was used as a filter to determine the average proportion of incident light that is scattered by DPPC LUVs during UV irradiation. To account for losses due to the reflection of incident light at cell surfaces, and differences in the refractive indicies of the solvents, measurements were also performed with hexane in the 5 mm cell under identical experimental conditions. A comparison of the photon rates from four independent sets of experiments shows that <5% of the incident light is scattered by DPPC LUVs. As a result, an upper limit was determined to give a range for the relative quantum efficiency of **1** in DPPC LUVs.

2.2.9. Differential scanning calorimetry (DSC) studies

Following MLV preparation protocols, DPPC MLVs and those containing **1** were prepared. Samples (7 μL) were hermetically sealed in 40 μL aluminum pans. Sample mass (pan, lid, and sample) was recorded before and after pressing to ensure no sample loss in the sealed pan. All samples were referenced to pans containing HEPES buffer. The scan rate employed was 2 °C/min and the temperature range was 10–60 °C.

2.2.10. Irradiation studies

LUV samples (A, B, C, and D) were diluted with buffer (ca. 15 mL, ca. 0.08 mM) and deoxygenated with argon for at least 15 min before being transferred to Pyrex test tubes. The tubes were loaded onto a rotating sample rack that was placed into a 2 L Pyrex beaker containing a cupric sulfate solution (100 mM) at constant temperature (20 ± 2 °C) to absorb shorter wavelengths of light (<320 nm) [24]. This assembly was then positioned into the photochemical reactor. Irradiations were performed in the following order: 30 s UV, 10 min vis, 30 s UV, and 10 min vis. Aliquots of the samples (1.5 mL) were separately transferred into the same quartz fluorescence cell, and their absorbance and fluorescence spectra were recorded before and after each irradiation. After the measurements, aliquots were discarded and the

cell was thoroughly cleaned with water and methanol, and then dried under a stream of argon before transferring the next aliquot. All measurements were performed in the dark and samples were covered during transport. To the final aliquots, 25 μL of a 10% Triton X-100 solution (v/v in buffer) was added to solubilize the LUVs to determine the fluorescence intensity representing 100% release of HPTS–DPX.

2.2.11. Data analysis

All recorded absorption and fluorescence spectra were baseline corrected to zero in a region where no absorbance or emission was observed (696–700 nm). The observed emission intensities (I_{obs}) for the spectra of samples C and D were corrected for primary ($f_p[A(\lambda_{413\,nm})]$, Eq. (4)), and secondary ($f_s[A(\lambda_{510\,nm})]$, Eq. (5)) inner filter effects (IFEs) from known procedures [25–27] using Eq. (6),

$$f_p[A(\lambda_{ex})] = \frac{10^{-A(\lambda_{ex})l_p}(10^{A(\lambda_{ex})\Delta l_p/2} - 10^{-A(\lambda_{ex})\Delta l_p/2})}{2.303A(\lambda_{ex})\Delta l_p} \quad (4)$$

$$f_s[A(\lambda_{em})] = \frac{10^{-A(\lambda_{em})l_s}(10^{A(\lambda_{em})\Delta l_s/2} - 10^{-A(\lambda_{em})\Delta l_s/2})}{2.303A(\lambda_{em})\Delta l_s} \quad (5)$$

$$I_{cor} = \frac{I_{obs}}{f_p[A(\lambda_{ex})]f_s[A(\lambda_{em})]} \quad (6)$$

where the distance from the point inside the cell at which fluorescence is observed to the entry and exit cell walls are assigned as l_p and l_s, respectively (0.5 cm), and Δl_p and Δl_s are the width of the emission and excitation light beams (ca. 0.35 cm). The absorbance of samples A and B at 413 nm and 510 nm ($A(\lambda_{413\,nm})$, and $A(\lambda_{510\,nm})$) were obtained from their respective absorption spectra. It should be noted that errors associated with the determination of Δl_p and Δl_s had little effect on the IFEs and the resulting corrected fluorescence intensities (I_{cor}). Following these corrections, the fluorescence intensity due solely to HPTS was determined for samples C and D, ensuring that artifacts, such as Raman emission of the solvent, light scattering, liposome photodegradation, and weak fluorescence from the isomers of **1**, were subtracted from the fluorescence spectra. This was obtained by subtracting the fluorescence spectrum of sample A from that of sample C (C–A) obtained before and after each irradiation. Similarly, the fluorescence spectrum for sample B was subtracted from that of sample D (D–B). Subsequently, the resulting subtracted spectra, C–A and D–B, were normalized to the spectrum recorded prior to irradiation at 510 nm to give spectra E and F, respectively. Finally, the net change due to the photoisomerization of **1** was calculated by subtracting the fluorescence spectra E from spectra F.

In addition, the percent release of HPTS from LUVs was calculated by comparing the fluorescence intensities observed from the subtracted spectra C–A, and D–B to that for the fluorescence intensity of the respective sample prior to irradiation and following the addition of Triton X-100 using Eq. (7),

$$\%\text{Release} = \frac{I - I_0}{I_{100} - I_0} \times 100 \quad (7)$$

where I is the corrected fluorescence intensity at 510 nm following a given irradiation, I_0 the corrected fluorescence prior to irradiation, and I_{100} is the corrected fluorescence intensity following the addition of Triton X-100.

3. Results

3.1. Liposome characterization

The size and lamellarity of the DPPC liposomes were determined by multi-angle laser light scattering (MALS) and fluorescence spectroscopy, respectively. In the MALS studies, two sets of DPPC LUV samples were prepared and measured to characterize LUV size and demonstrate the reproducibility of our preparation protocols for producing LUVs with relatively uniform size. The first set of samples was extruded through membrane filters with a pore size of 0.2 μm, and a second set was extruded through 0.4 μm filters. From our measurements and analysis, Zimm plots obtained using a spherical model gave radii for the 200 and 400 nm DPPC LUVs of 103.1 ± 4.9 nm and 207.2 ± 4.4 nm, respectively.

To measure the liposome lamellarity, melittin, an amphiphilic peptide from bee venom, was used as a lytic agent to induce release of encapsulated compounds from the liposomes [28–30]. This peptide has been shown to only disrupt the outermost lamella of liposomes, such that it will remove successive lamella of MLVs with multiple additions. To a sample of 400 nm DPPC liposomes encapsulating HPTS–DPX, melittin was added in sequential 10 μL aliquots. The fluorescence intensity of HPTS at 510 nm was measured after each addition (Fig. 1) until the fluorescence intensity reached a plateau (I_{Total}). This intensity represents the release of HPTS from the total liposome mixture, which may include both LUVs and MLVs. The total volume of

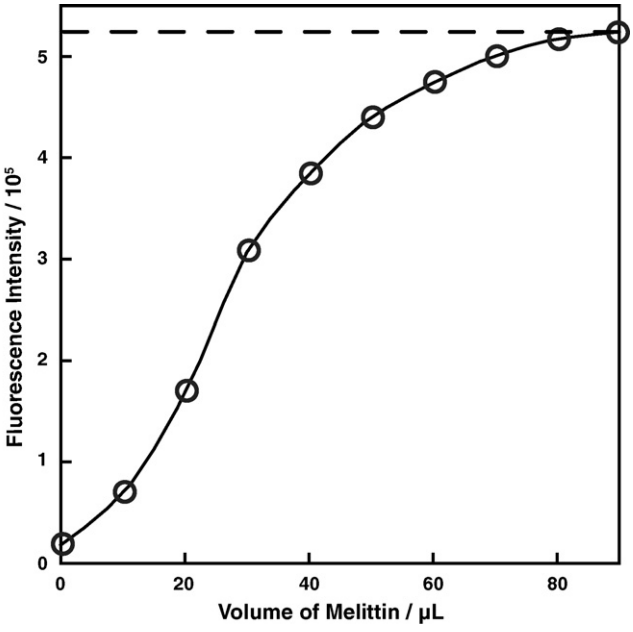

Fig. 1. Determining the lamellarity of 400 nm DPPC liposomes. Changes in the fluorescence intensity of HPTS at 510 nm were recorded following the addition of 10 μL aliquots of a 100 μM melittin stock solution to the liposome mixture (i.e. LUVs and MLVs). The dashed line represents an extrapolation from the plateau region used to determine the value of I_{Total}.

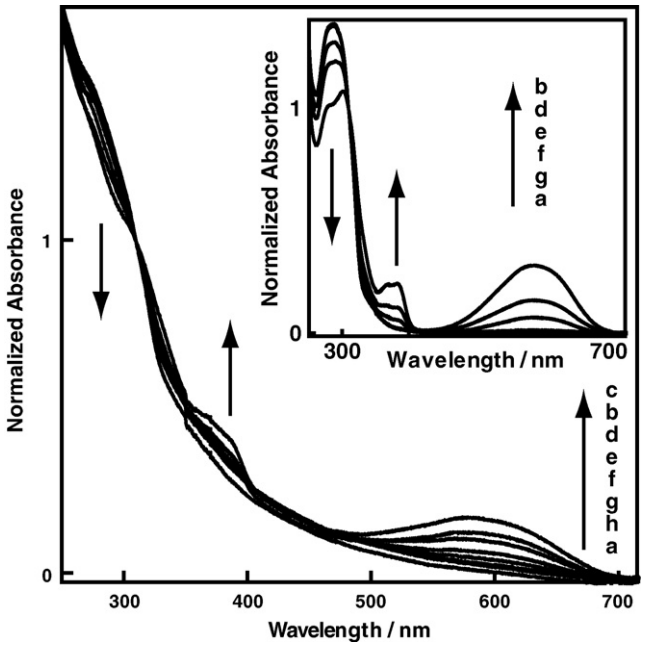

Fig. 2. Normalized absorption spectra of **1** in 100 nm DPPC LUVs prior to irradiation (a) and after irradiation with UV or visible light in the following sequence: (b) 30 s of UV, (c) 2 min of UV, (d) 90 s of vis, (e) 3 min of vis, (f) 5 min of vis, (g) 10 min of vis and (h) 15 min of vis. The inset is normalized absorption spectra of **1** in chloroform under identical experimental conditions.

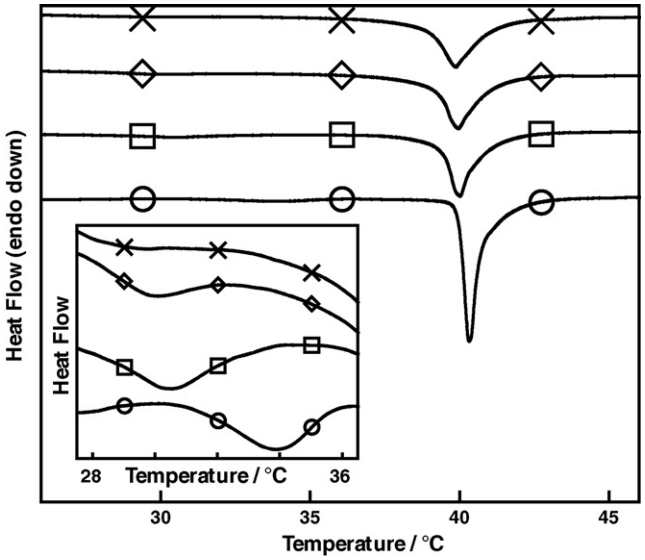

Fig. 3. DSC curves of DPPC MLVs in the absence (◯) and presence of **1** with various mole ratios (**1**:DPPC): 1:4 (□), 1:3 (◊), 1:2 (×). The inset is an expansion of the pretransitional region.

melittin required to reach this plateau was then added to an identical sample in one aliquot and the fluorescence intensity (I_{LUV}) was recorded. This intensity represents the release of HPTS from only LUVs. The ratio of these intensities (I_{LUV}/I_{Total}) gives the ratio of LUVs in the total liposome mixture and was found to be 0.987 ± 0.005.

3.2. Absorption studies

Absorption spectra were recorded to characterize the inclusion and photochromism of **1** in DPPC LUVs. Compound **1**, predominantly as the photoisomer **1o**, was included in the lipid bilayer of LUVs with a diameter of 100 nm. LUVs of this size were prepared to reduce background absorbance due to light scattered by these supramolecular assemblies. Upon irradiation with broadband UV light, the colorless sample turned blue and an increase in absorbance was observed at 380 and 580 nm with a slight, concomitant decrease in the 280 nm region (Fig. 2). Further, the isosbestic point observed at 310 nm is a strong indication that only two interconverting species are present in solution [31]. Similar results were also observed for **1** in chloroform (inset of Fig. 2) and are consistent with the formation of **1c** [14,16]. The deconvolution of a broad shoulder at 280 nm, clearly observed in chloroform, was not resolvable in DPPC LUVs due to light scattering. Upon irradiation of the DPPC LUVs with visible light, the absorption bands due to the formation of **1c** reverted back to those of **1o**, demonstrating that photoisomerization is completely reversible. In addition, the longer irradiation times required for the conversion of **1c** to **1o** in both DPPC LUVs and chloroform are consistent with the fact that the quantum yield for the ring-closing reaction is 45-fold greater than the ring-opening reaction in hexane (0.58 versus 0.013 [16], respectively).

The relative quantum efficiency for the ring-closing reaction of **1** in DPPC LUVs was determined by comparing its quantum efficiency with **1** in hexane. The quantum efficiency of **1** in LUVs was found to be (22 ± 7)-fold smaller than in hexane. The large standard deviation calculated for this result was primarily due to errors associated with measuring small changes in absorbance that were observed for **1** in DPPC LUVs. Further, this ratio represents a lower limit for the relative quantum efficiency because a proportion of the total number of incident photons are scattered by the LUVs. To obtain an upper limit for the relative quantum efficiency the proportion of incident light scattered by LUVs was quantified. Our results show that <5% of the incident UV light is scattered by DPPC LUVs. Given that the standard deviation for the lower limit of the relative quantum efficiency is larger than 5% of the mean, the upper and lower limits are best expressed as a standard deviation of the mean.

3.3. Differential scanning calorimetry studies

The thermotropic phase behavior of MLVs composed of pure DPPC and in mole ratios of 1:4, 1:3 and 1:2 (**1**:DPPC) were recorded using DSC to determine the relative inclusion and location of **1** in the lipid bilayer. Initially, similar LUV samples were measured, however, no clear phase transitions were observed due to the relatively low concentration of DPPC. The DSC curve for pure DPPC MLVs (Fig. 3) shows its signature main phase transition temperature (T_m) with a narrow temperature range at half its maximum ($\Delta T_{1/2}$). A small shift to lower temperature and broadening of the main phase transition is observed for MLVs with increasing mole ratios of **1** relative to pure DPPC MLVs (Table 1). These observations are consistent with those observed from similar studies that have investigated the effect of additives on the thermotropic phase behavior of DPPC MLVs [32,33].

Table 1
The main phase transition temperature (T_m) and temperature difference at half maximum ($\Delta T_{1/2}$) for DPPC MLVs with various mole ratios of **1**

Mole ratio (**1**:DPPC)	T_m (°C)	$\Delta T_{1/2}$ (°C)
0:1	40.28 ± 0.03	0.59 ± 0.11
1:4	39.99 ± 0.04	1.18 ± 0.23
1:3	39.95 ± 0.03	1.26 ± 0.10
1:2	39.88 ± 0.04	1.37 ± 0.08

Less noticeable is a weak yet signature pretransition at ca. 34 °C for pure DPPC MLVs (inset of Fig. 3). This pretransition also shifts to lower temperature and virtually disappears with increasing mole ratios of **1**. The difference in T_m and $\Delta T_{1/2}$ for samples with a **1**:DPPC from 1:4 to 1:2 is relatively small compared with the difference observed between pure DPPC and 1:4.

3.4. Irradiation studies

HPTS–DPX was chosen as probe system to monitor the changes in the permeability of 400 nm LUVs incorporating **1**, since HPTS undergoes efficient self-quenching at moderate concentrations and in the presence of the collisional quencher DPX [34,35]. To minimize any experimental artifacts that may affect the observed fluorescence intensity, three controls were prepared (i.e. DPPC LUVs (sample A), and those containing **1** (sample B) or HPTS–DPX (sample C)) in addition to LUVs incorporating **1** and encapsulating HPTS–DPX (sample D). These artifacts may include but are not limited to the leakage of HPTS from the LUVs, fluorescence of **1o**, Raman emission of the solvent, and light scattered by the LUVs. Photoinduced changes in membrane permeability were assessed by monitoring changes in the fluorescence of HPTS upon photocycling **1** between the two photoisomers using UV and visible light. The mole ratio employed was 1:3 (**1**:DPPC) as increasing the concentration of **1** in our preparations did not significantly enhance the concentration of **1** included in the liposomes as demonstrated from the DSC studies. To be certain that the LUVs prepared were stable throughout the irradiation studies, a 25 μL aliquot of 10% (v/v) Triton X-100 was added to lyse the LUVs after the irradiations were finished. Triton X-100 is a lipid soluble surfactant that will effectively lyse the liposome membrane resulting in complete release of encapsulated HPTS and relief from the quenching of its fluorescence. As a result, this procedure also allowed for the determination of the total fluorescence so that the percentage of HPTS released could be calculated. It is important to note that we intentionally performed these studies below the T_m of DPPC (ca. 41 °C [33]) for three important reasons. First, similar studies [4,7,11] have shown that photorelease is generally limited to the gel phase since bilayers in the liquid-crystalline phase are better able to adapt to changes in the molecular geometry of the photochrome arising from their isomerization. Second, liposomes around T_m are significantly more permeable and substantial HPTS leakage from DPPC LUVs was observed when these samples were placed in the dark. Third, liposomes used in biomedical applications such as drug delivery are predominantly administered in the gel phase [1,2].

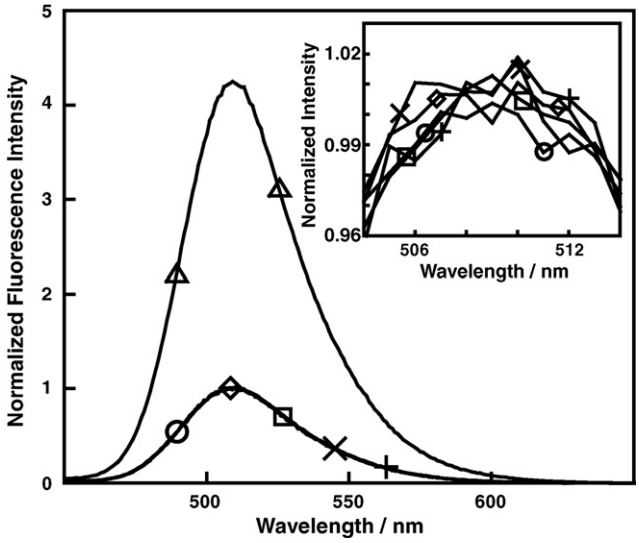

Fig. 4. Corrected and normalized fluorescence spectra of HPTS for 400 nm DPPC LUVs in the absence of **1** prior to irradiation (◯), after irradiation with UV or visible light in the following sequence: 30 s of UV (□), 10 min of vis (◊), 30 s of UV (×), 10 min of vis (+), and following addition of a 25 μL aliquot of 10% (v/v) Triton X-100 (△). The inset is an expansion of the spectra near the maxima.

Fluorescence spectra were recorded for all samples before and after each irradiation interval. The spectra for samples A and B served as controls for the spectra recorded for samples C and D, respectively. After the necessary baseline and IFE corrections were applied to all the spectra, the fluorescence spectra of sample A were subtracted from the fluorescence spectra of sample C and then normalized to the spectrum prior to irradiation at 510 nm to give spectra E (Fig. 4). Similarly, the fluorescence spectra of sample B were subtracted from the fluorescence spec-

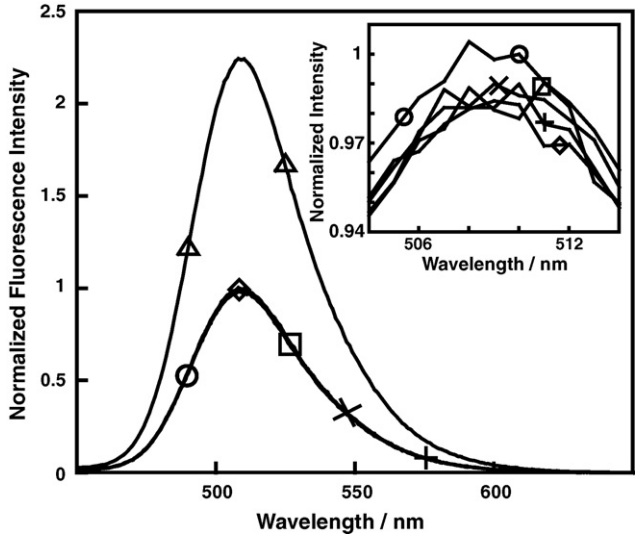

Fig. 5. Corrected and normalized fluorescence spectra of HPTS for 400 nm DPPC LUVs in the presence of **1** with a mole ratio of 1:3 (**1**:DPPC) prior to irradiation (◯), after irradiation with UV or visible light in the following sequence: 30 s of UV (□), 10 min of vis (◊), 30 s of UV (×), 10 min of vis (+), and following addition of a 25 μL aliquot of 10% (v/v) Triton X-100 (△). The inset is an expansion of the spectra near the maxima.

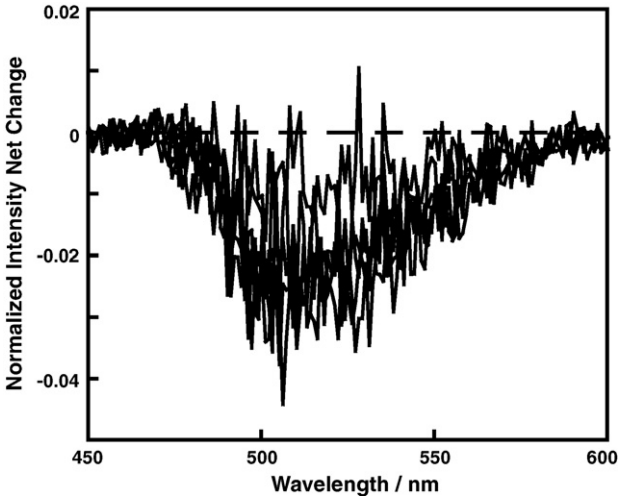

Fig. 6. The net change in the fluorescence spectra of HPTS due to the photoisomerization of **1** in 400 nm DPPC LUVs. The normalized fluorescence spectra of DPPC LUVs in the absence of **1** (Fig. 4) were subtracted from those in the presence of **1** with a mole ratio of 1:3 (**1**:DPPC) (Fig. 5). The dashed line represents no net change.

tra of sample D and then normalized to give spectra F (Fig. 5). A net change in the fluorescence intensity of HPTS due solely to the photoisomerization of **1** was obtained by subtracting the fluorescence spectra of E from the fluorescence spectra of F (Fig. 6). From repetitive experiments, significant changes in the fluorescence spectra of HPTS for DPPC LUVs containing **1** were not observed following the irradiation intervals. Consequently, an average net change of -0.019 ± 0.012 was obtained (Fig. 7).

As an alternative method of analysis, the percent release of HPTS for samples C and D following irradiations were also calculated by comparing these changes in fluorescence intensity at 510 nm to that following the addition of Triton X-100

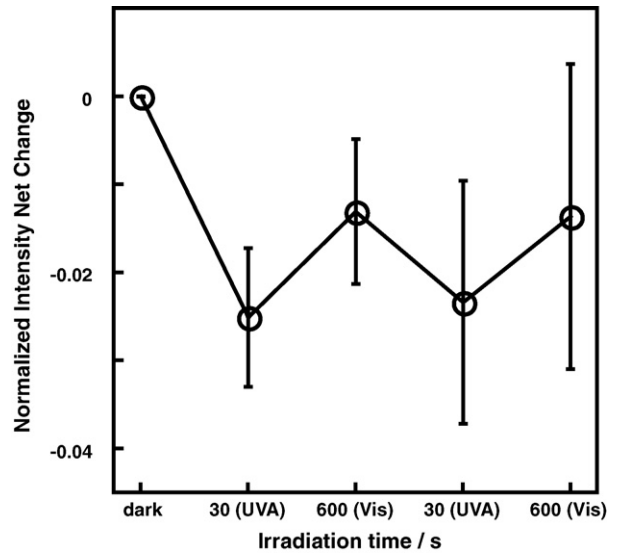

Fig. 7. The net change in the fluorescence of HPTS at 510 nm due to the photoisomerization of **1** in 400 nm DPPC LUVs with a mole ratio of 1:3 (**1**:DPPC) prior to and after irradiation with UV or visible light. The error bars represent the standard deviations of the calculated means.

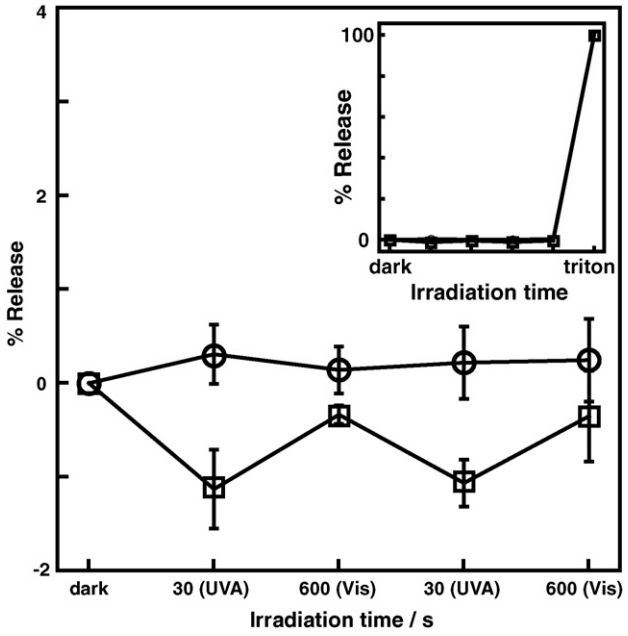

Fig. 8. The percent release of HPTS from 400 nm DPPC LUVs in the absence (◯) and presence of **1** (□) prior to and after irradiation with UV or visible light. The error bars represent the standard deviations of the calculated means. The inset includes the maximal release which was determined following the addition of a 25 μL aliquot of 10% (v/v) Triton X-100.

(Fig. 8). LUVs not incorporating **1** showed a slight increase in HPTS emission ($0.23 \pm 0.31\%$) following the various irradiation intervals whereas those incorporating **1** showed a slight decrease ($-0.72 \pm 0.49\%$). As a result, an apparent release was not observed following the irradiation of LUVs incorporating **1**.

4. Discussion

The main objectives in this study are to establish that **1** is included in the lipid bilayer, determine its relative location within the membrane, and show that its photochromism is conserved. These characteristics are important to the development of a photochromic liposomal system in which membrane permeability can be completely controlled with light. The use of photochromic compounds to affect the permeability of a lipid bilayer has been shown for azobenzene [7,8] and spiropyran [9–11] systems. However, in all cases these compounds were thermally reversible which limits complete photocontrol over the release of encapsulated compounds. A thermally irreversible system will allow for improved regulation of the delivered dosage. Before employing synthetically more challenging dithienylethene derivatives with complementary lipid-like structures that will potentially cause a greater disruption to the lipid bilayer, it is important that we establish our primary objectives with the analogous parent system, including the development of protocols for determining quantum efficiencies in LUVs and assessing membrane permeability.

To establish the inclusion of **1** in the bilayer of LUVs and conservation of its photochromism, absorption spectra were recorded for DPPC LUVs containing **1** (Fig. 2). LUVs with a diameter of 100 nm were prepared since LUVs with smaller

diameters scatter light in the UV–vis region less efficiently resulting in lower background absorbance [1]. Similar to studies in organic solvents, **1** was predominantly in the **1o** form prior to irradiation since no absorption due to **1c** was detected. Upon irradiation with UV light, an increase in absorbance at 380 and 580 nm, and a slight, concomitant decrease at 280 nm was observed, confirming the presence of **1c** in LUVs. Following the conversion of **1c** to **1o** with visible irradiation, absorption at 380 and 580 nm decreased, and absorption in the 280 nm region increased, which clearly demonstrates that the photoisomerization of **1** in the gel phase of DPPC LUVs is completely reversible. As **1** is unlikely located in the aqueous compartment of liposomes due to its low solubility in water, we have concluded that **1** is incorporated in the lipid bilayer of a liposome and have shown that its photochromism is conserved.

In general, the determination of reaction quantum yields in heterogeneous systems has been challenging primarily because the number of photons scattered by the suspended particulates has been experimentally difficult to quantify [36,37]. Unfortunately, in some cases the reported quantum yields are in reality apparent quantum yields and effectively lower limits of the true quantum yield. To circumvent these uncertainties, methods have been developed that employ standard secondary actinometers. For example, in the area of heterogeneous photocatalysis, the relative photonic efficiencies for the degradation of organic pollutants in aqueous suspensions of titanium dioxide are often compared with the degradation of phenol under identical experimental conditions [36]. In contrast, few methods have been developed for the determination of photoisomerization quantum yields in organized systems [38]. Time-resolved absorption spectroscopy has been used to qualitatively estimate photoisomerization efficiencies for cyanine dyes in LUVs and thin polymer films when correlated with the quantum yields for competitive deactivation pathways, such as fluorescence and intersystem crossing [39]. In this study, we have developed a new method to determine a range for the relative quantum efficiency for the ring-closing reaction of **1** in DPPC LUVs by comparing its quantum efficiency to **1** in hexane. The quantum efficiency of **1** in LUVs was found to be (22 ± 7)-fold smaller than in hexane. This result is consistent with the report on cyanine dyes in LUVs, which concluded that the photoisomerization process was hindered by the more viscous nature of the lipid bilayer compared with organic solvent [39]. As well, the rigid medium of a thin polymer film was shown to completely inhibit photoisomerization such that the only observable intermediate was the triplet state of the cyanine dye [39]. In a similar study, the effect of solvent viscosity on the photoisomerization quantum yield of a diarylethene derivative was examined [40]. These studies also showed that cyclization yields decreased with an increase in the viscosity of the local environment. Consequently, the smaller quantum efficiency observed for the ring-closing reaction of **1** in DPPC LUVs compared with hexane is due to the more restrictive and rigid environment posed by the lipid bilayer in the gel phase. We are currently developing a separation protocol to isolate the photoisomers of **1** from the lipid matrix so that high-performance liquid chromatography can be used to determine quantum efficiencies in DPPC LUVs with better precision, analogous to protocols reported for the separation of arylstilbazolium ligands from DNA [38].

To obtain a better understanding on the relative location of **1** within the lipid bilayer, DSC was employed to investigate changes in the phase transition temperatures of pure DPPC MLVs compared with those containing **1**. Surprisingly, previous reports on the inclusion of photochromic compounds in liposomes have not investigated thermotropic phase behaviors. MLVs were prepared to increase the concentration of the lipids and additives, thus enhancing the signal to noise ratio of the DSC curves. In addition, the thermotropic phase behavior of DPPC MLVs are similar to LUVs [33,41,42]. When additives are incorporated into the lipid bilayer of a liposome, the phase behavior of the liposome is altered. This effect on the gel-to-liquid crystalline phase transition has been studied in DPPC liposomes for over 100 hydrophobic small molecules using DSC [32,33]. Four distinctive profiles have been assigned to the interaction of these molecules within specific regions of the bilayer. In particular, the type A profile is characterized by a shift in T_m to a lower temperature and an increase in the $\Delta T_{1/2}$ upon the addition of small molecules. More specifically, this profile suggests that the additives are partially buried in the hydrocarbon core of the bilayer, interacting primarily with the C2–C8 methylene region of the acyl chains of DPPC. Using this analysis, the relative location of **1** in the lipid bilayer can be determined by monitoring changes in the DSC curves with increasing concentrations of the photochrome. In our studies, DPPC MLVs containing **1** were prepared at mole ratios of 1:4, 1:3 and 1:2 (**1**:DPPC). A comparison of the DSC curves for pure DPPC and those containing **1** with increasing mole ratios showed a decrease in T_m and an increase in $\Delta T_{1/2}$. Although the changes in T_m were relatively small between pure DPPC with those containing **1**, a highly reproducible decrease was observed. Also, a significant broadening of the transition shown by the increase in $\Delta T_{1/2}$ was observed when comparing pure DPPC with 1:4. These observations best represent the type A profile, which suggests that **1** is primarily interacting with the C2–C8 methylene region of the phospholipid hydrocarbon chains of DPPC LUVs. In addition, the DSC curve for pure DPPC showed a signature pretransition at ca. 34 °C, for the transition between two specific gel phases (i.e. lamellar gel-to-ripple phase [33]). This transition shifted to lower temperatures and practically disappeared with the inclusion of **1**. This disappearance in the pretransition upon the inclusion of additives has been reported by others [32,33,43,44] and clearly indicates that **1** is interacting with the lipid bilayer.

Having established the relative location of **1** within the lipid bilayer, the effect of its photochromism on the permeability of the bilayer was investigated. Our initial hypothesis was that the photoisomerization of **1** would not lead to a significant disruption in the local lipid order within the bilayer. This hypothesis was based primarily on the noncomplementary nature of **1** when compared with DPPC. Also, changes in the molecular geometry of **1** are potentially too small to disrupt lipid organization considering the photoisomerization of **1** has been established in the single-crystalline phase [16]. As a result, no significant effect on the permeability of the membrane was anticipated. Nevertheless,

before using synthetically more challenging dithienylethene analogs, it was important to develop our protocols for evaluating the effect of the photoisomerization of **1** on membrane permeability.

Membrane permeability studies were performed by monitoring changes in the fluorescence intensity of HPTS upon switching between the photoisomers **1o** and **1c**. An increase in fluorescence intensity would indicate that HPTS was released from the LUVs into the bulk aqueous phase where its fluorescence is relatively free from collisional quenching. As a result, HPTS release would suggest that the increase in membrane permeability is due to a significant disruption in the local lipid order resulting from changes in the molecular geometry of **1** accompanying photoisomerization. Our results clearly show that a significant change in fluorescence intensity was not observed following sequential irradiations of **1** with UV and visible light. A large increase in HPTS fluorescence was observed upon the addition of Triton X-100, which indicates that the liposomes were stable during the study. Upon closer inspection of the data and after applying necessary baseline and IFE corrections, a net change in the fluorescence intensity of HPTS induced by the photoisomerization of **1** was slightly negative (-0.019 ± 0.012) which initially suggested that the controls were more permeable than the sample containing **1**. To confirm this result, an alternative method of analysis was also performed by determining the percent release of HPTS from LUVs. LUVs not incorporating **1** showed a slight increase in HPTS emission ($0.23 \pm 0.31\%$) following the various irradiation intervals whereas those incorporating **1** showed a slight decrease ($-0.72 \pm 0.49\%$). As the changes in the fluorescence intensity of HPTS induced by the photoisomerization of **1** were small and negative, we carefully considered all possible sources of experimental error to determine if these changes were due to inherent experiment artifacts. Although these experiments were repeated multiple times to minimize random errors, we were unable to determine the reasoning for the slight decrease. In any case, these results with their associated errors clearly illustrate that we are very close to zero and most likely at the detection limits of our experimental setup. Consequently, the release of encapsulated HPTS was not observed following the irradiation of LUVs incorporating **1**, which supports our hypothesis that the photoisomerization of **1** does not lead to a large disruption in the local lipid order within the bilayer.

A possible explanation for the lack of significant increases in membrane permeability may be the nonamphiphilic nature of **1**. Previously reported azobenzene [7] and spiropyran [11] derivatives that did show modest levels of fluorophore release possessed a typical lipid-like amphiphilic structure. The former derivative covalently incorporated the azobenzene moiety into the acyl chains of a DPPC lipid whereas the latter conjugated the photochromic moiety to a long alkyl chain with a terminal, charged triethylammonium substituent. Presumably, these derivatives were better able to organize themselves within the lipid bilayer through significant intermolecular interactions with the hydrophobic acyl chains and hydrophilic zwitterionic head groups of the DPPC lipids. Hence, photoisomerization likely produced a larger disruption in the local lipid order. Even though the relative concentrations of **1** in the LUVs were high, another possible reason may be that the changes in the molecular geometry of **1** accompanying photoisomerization are not large enough to significantly disrupt lipid organization within the bilayer. To improve photocontrol over membrane permeability, derivatives of **1** that undergo much larger changes in molecular geometry will be essential, such as a recently reported derivative containing bulky phenylethynyl substituents in place of the methyl groups of **1** [45]. We are currently developing new dithienylethene derivatives that will address these key issues.

In summary, we have shown that photochrome **1** is included in the lipid bilayer of DPPC liposomes, primarily located within the C2–C8 methylene region of the lipid acyl chains, and its photoisomerization is completely reversible, although hindered due to the more restrictive and rigid environment posed by the lipid bilayer. The release of encapsulated HPTS is not observed following the irradiation of LUVs incorporating **1**, which strongly suggests that the photoisomerization of **1** does not lead to a significant disruption in the local lipid order within the bilayer.

Acknowledgements

This work was supported by the Natural Sciences and Engineering Research Council (NSERC) of Canada and the University of Regina. The authors would like to thank T.E.S. Dahms and K. Asghari for the use of their instrumentation, and T.M. Fyles for helpful discussions.

References

[1] D.D. Lasic, Liposomes: From Physics to Applications, Elsevier Science, New York, 1993.
[2] D.D. Lasic, Trends Biotechnol. 16 (1998) 307–321.
[3] T. Lian, R.J.Y. Ho, J. Pharm. Sci. 90 (2001) 667–680.
[4] P. Shum, J.-M. Kim, D.H. Thompson, Adv. Drug Deliv. Rev. 53 (2001) 273–284.
[5] B. Bondurant, A. Mueller, D.F. O'Brien, Biochim. Biophys. Acta 1511 (2001) 113–122.
[6] A. Mueller, B. Bondurant, D.F. O'Brien, Macromolecules 33 (2000) 4799–4804.
[7] R.H. Bisby, C. Mead, C.G. Morgan, Biochem. Biophys. Res. Commun. 276 (2000) 169–173.
[8] Y. Lei, J.K. Hurst, Langmuir 15 (1999) 3424–3429.
[9] R.F. Khairutdinov, J.K. Hurst, Langmuir 17 (2001) 6881–6886.
[10] A. Koçer, M. Walko, W. Meijberg, B.L. Feringa, Science 309 (2005) 755–758.
[11] Y. Ohya, Y. Okuyama, A. Fukunaga, T. Ouchi, Supramol. Sci. 5 (1998) 21–29.
[12] R.F. Khairutdinov, K. Giertz, J.K. Hurst, E.N. Voloshina, N.A. Voloshin, V.I. Minkin, J. Am. Chem. Soc. 120 (1998) 12707–12713.
[13] S.L. Gilat, S.H. Kawai, J.-M. Lehn, Chem. Eur. J. 1 (1995) 275–284.
[14] M. Irie, Chem. Rev. 100 (2000) 1685–1716.
[15] K. Uchida, M. Irie, Photochromism of diarylethene derivatives, in: W. Horspool, F. Lenci (Eds.), CRC Handbook of Organic Photochemistry and Photobiology, vol. 35, CRC Press, London, 2004, pp. 1–14.
[16] M. Irie, T. Lifka, S. Kobatake, N. Kato, J. Am. Chem. Soc. 122 (2000) 4871–4876.
[17] K.E. Maly, M.D. Wand, R.P. Lemieux, J. Am. Chem. Soc. 124 (2002) 7898–7899.
[18] T.J. Wigglesworth, N.R. Branda, Adv. Mater. 16 (2004) 123–125.
[19] R. Lantz, A. Hornfeldt, Chem. Scripta 2 (1972) 9–15.
[20] R. Pereira, B. Iglesias, A.R. de Lera, Tetrahedron 57 (2001) 7871–7881.

[21] C.G. Hatchard, C.A. Parker, Proc. R. Soc. (London) A235 (1956) 518–536.
[22] F. Szoka Jr., D. Papahadjopoulos, Annu. Rev. Biophys. Bioeng. 9 (1980) 467–508.
[23] A.M. Braun, M.-T. Maurette, E. Oliveros, Photochemical Technology, Wiley, Chichester, 1991.
[24] M. Montalti, A. Credi, L. Prodi, M.T. Gandolfi, Handbook of Photochemistry, CRC Press, Boca Raton, 2006.
[25] B. Birdsall, R.W. King, M.R. Wheeler, C.A. Lewis Jr., S.R. Goode, R.B. Dunlap, G.C.K. Roberts, Anal. Biochem. 132 (1983) 353–361.
[26] J.F. Holland, R.E. Teets, P.M. Kelly, A. Timnick, Anal. Chem. 49 (1977) 706–710.
[27] M. Kubista, R. Sjoback, S. Eriksson, B. Albinsson, Analyst 119 (1994) 417–419.
[28] T. Benachir, M. Lafleur, Biochim. Biophys. Acta 1235 (1995) 452–460.
[29] J.R. Pik, H.G. Lawford, Can. J. Biochem. 10 (1980) 996–1003.
[30] S. Rex, G. Schwarz, Biochemistry 37 (1998) 2336–2345.
[31] D.C. Harris, Quantitative Chemical Analysis, W.H. Freeman, New York, 1991.
[32] M.K. Jain, N.M. Wu, J. Membr. Biol. 34 (1977) 157–201.
[33] R.N.A.H. Lewis, R.N. McElhaney, The Mesomorphic phase behavior of lipid bilayers, in: P. Yeagle (Ed.), The Structure of Biological Membranes, CRC Press, London, 1992, pp. 73–155.
[34] D.L. Daleke, K. Hong, D. Papahadjopoulos, Biochim. Biophys. Acta 1024 (1990) 352–366.
[35] S.G. Schulman, C. Shangxian, B. Fenglian, M.J.P. Leiner, L. Weis, O.S. Wolfbeis, Anal. Chim. Acta 304 (1995) 165–170.
[36] N. Serpone, J. Photochem. Photobiol., A 104 (1997) 1–12.
[37] L. Sun, J.R. Bolton, J. Phys. Chem. 100 (1996) 4127–4134.
[38] B. Juskowiak, M. Chudak, Photochem. Photobiol. 79 (2004) 137–144.
[39] M. Krieg, M.B. Srichai, R.W. Redmond, Biochim. Biophys. Acta 1151 (1993) 168–174.
[40] H. Miyasaka, T. Nobuto, M. Murakami, A. Itaya, N. Tamai, M. Irie, J. Phys. Chem. A 106 (2002) 8096–8102.
[41] D. Lichtenberg, M. Menashe, S. Donaldson, R.L. Biltonen, Lipids 19 (1984) 395–400.
[42] N. Düzgüneş, J. Wilschut, K. Hong, R. Fraley, C. Perry, D.S. Friend, T.L. James, D. Papahadjopoulos, Biochim. Biophys. Acta 732 (1983) 289–299.
[43] S. Ali, S. Minchey, A. Janoff, E. Mayhew, Biophys. J. 78 (2000) 246–256.
[44] C. Valenta, A. Steininger, B.G. Auner, Eur. J. Pharm. Biopharm. 57 (2004) 329–336.
[45] K. Morimitsu, S. Kobatake, M. Irie, Tetrahedron Lett. 45 (2004) 1155–1158.